

Nonlinear optical susceptibilities $\chi^{(2)}$ of nitridosilicate powders

Holger Lutz^a, Sven Joosten^a, Jochen Hoffmann^a, Petra Lehmeier^a,
Alois Seilmeier^a, Henning A. Höpfe^{b,c}, Wolfgang Schnick^{b,*}

^aPhysikalisches Institut, Universität Bayreuth, D-95440 Bayreuth, Germany

^bDepartment Chemie, Ludwig-Maximilians-Universität München, Butenandtstraße 5-13 (D), D-81377 München, Germany

^cInorganic Chemistry Laboratory, University of Oxford, South Parks Road, Oxford OX1 3QR, UK

1. Introduction

The frequency conversion of coherent radiation via parametric devices like optical parametric oscillators and frequency doublers has found increasing attention in recent years. New materials with high nonlinear optical susceptibilities and high damage thresholds are of special interest for such devices. Materials with noncentrosymmetric crystal structures like nitridosilicates with their superior mechanical properties and their high thermal stability are attractive candidates. No investigations of the nonlinear optical properties of nitridosilicates have been reported in the literature as yet.

Most novel materials are only available in powder form and standard techniques for the determination of the susceptibility tensor cannot be used. Initial information is available from powder methods which measure an average of the tensor components. A frequently used powder method is the Kurtz–Perry-Method [1] in which light at the fundamental frequency penetrates the sample and generates a signal at the second harmonic (SH) frequency.

This technique suffers from the fact that phase matching in the powder crystallites may occur and the results strongly depend on the relation between the—in most of the cases—unknown coherence length and the size of the crystallites.

To avoid this problem, a method using a total reflection geometry has attracted increasing attention in recent years which is called SHEW-method (Second Harmonic Wave generated by an Evanescent Wave) [2,3]. Laser light is totally reflected at an interface between a material with high refractive index and the sample under investigation. The second harmonic signal generated in this geometry is proportional to a weighted average of all tensor components of the material [4].

In this paper the Kurtz–Perry and the SHEW-method are used to measure the optical nonlinearity $\chi_{\text{eff}}^{(2)}$ of nitridosilicates. Simultaneously, we obtain information on the refractive indices from the SHEW investigations. After a short review of the SHEW technique we present experimental results. The averaged effective Figure of Merit $M_{\text{eff}} = d_{\text{eff}}^2/n_{2\omega}n_{\omega}^2$ with $d_{\text{eff}} = 0.5\chi_{\text{eff}}^{(2)}$, which is a measure for the efficiency of the nonlinear interaction process, is found to be of the same order of magnitude as that of LiIO_3 in the most efficient samples and very high refractive indices between 2 and 3 result from our findings.

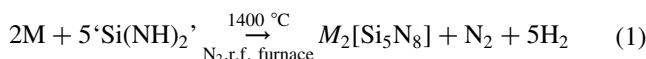
* Corresponding author. Tel.: +49-89-2180-77436; fax: +49-89-2180-77440.

E-mail address: wolfgang.schnick@uni-muenchen.de (W. Schnick).

2. Experimental section

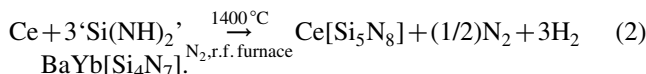
2.1. Preparation of the powder samples

$M_2[\text{Si}_5\text{N}_8]$ with $M = \text{Ca}, \text{Sr}, \text{Ba}$. A mixture of the respective alkaline earth metal (Sr: 70.0 mg, 0.799 mmol, ABCR, 99.95%, Ba: 120.1 mg, ABCR, 99.9%, 0.874 mmol, Ca: 32.0 mg, 0.798 mmol, ABCR, 99.997%) and $\text{Si}(\text{NH})_2$ (116.0 mg, 2.00 mmol) [5] was thoroughly mixed under argon atmosphere in a glove box and transferred into a tungsten crucible positioned in a water-cooled silica glass reactor of a radiofrequency furnace (type IG 10/200 Hy, frequency: 200 kHz, electrical output: 0–12 kW, Hüttinger, Freiburg) [6,7]. The reaction mixture was heated under a pure nitrogen atmosphere (purified by silica gel, potassium hydroxide, molecular sieve, P_4O_{10} , and a BTS catalyst) to 900 °C within 5 min, maintained at that temperature for 25 min, heated to 1600 °C within 12 h, held there for 8 h, and subsequently cooled to 1000 °C within 3 h. Finally, the product was quenched to room temperature. This reaction (1) yielded single-phase $M_2[\text{Si}_5\text{N}_8]$ with $M = \text{Ca}, \text{Sr}, \text{Ba}$ as coarsely crystalline colorless powders. Excess metal condensed on the inner surface of the water-cooled reactor.

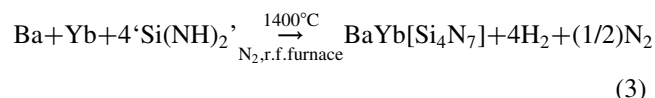


$M = \text{Ca}, \text{Sr}, \text{Ba}$

$\text{Ce}[\text{Si}_3\text{N}_5]$. A mixture of cerium metal (35.2 mg, 0.251 mmol, ABCR, 99.95%) and ‘ $\text{Si}(\text{NH})_2$ ’ (59.6 mg, 1.03 mmol) [5] was thoroughly mixed under argon atmosphere in a glove box and transferred into a tungsten crucible positioned in a water-cooled silica glass reactor of the previously mentioned radiofrequency furnace [6,7]. The reaction mixture was heated under a pure nitrogen atmosphere to 1000 °C within 5 min, maintained at that temperature for 25 min, heated to 1500 °C within 12 h, and subsequently cooled to 1200 °C within 6 h. Finally, the product was quenched to room temperature. This reaction (2) yielded single-phase $\text{Ce}[\text{Si}_3\text{N}_5]$ as a coarsely crystalline yellowish powder.



The synthesis of $\text{BaYb}[\text{Si}_4\text{N}_7]$ was performed in a radiofrequency furnace according to Eq. (3)



Under argon a mixture of 30.4 mg (0.523 mmol) silicon diimide [5] and 17.4 mg (0.127 mmol) barium metal (ABCR, 99.9%) and 23.0 mg (0.133 mmol) ytterbium metal (ABCR, 99.9%) were transferred into a tungsten crucible. The latter was then heated under nitrogen to

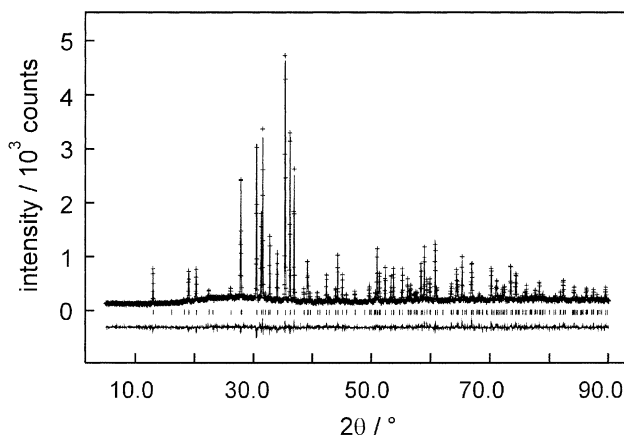


Fig. 1. Observed (crosses) and calculated (line) X-ray powder diffraction pattern ($\text{Cu K}\alpha_1$ radiation) as well as the difference profile of the Rietveld refinement of $\text{Sr}_2[\text{Si}_5\text{N}_8]$. The row of vertical lines indicates possible peak positions of $\text{Sr}_2[\text{Si}_5\text{N}_8]$.

1000 °C within 5 min in the water-cooled silica glass reactor of the radiofrequency furnace [6,7]. After 25 min the crucible was heated to 1600 °C within 12 h and held at this temperature for another 3 h. Then, the mixture was cooled to 1000 °C within 3 h. Subsequent quenching to room temperature within 30 min yielded single phase $\text{BaYb}[\text{Si}_4\text{N}_7]$. Excess barium or ytterbium metal evaporated off the reaction mixture and condensed at the inner surface of the water-cooled silica glass reactor. $\text{BaYb}[\text{Si}_4\text{N}_7]$ was obtained as a coarsely crystalline, yellowish powder.

The purity of our samples was checked by X-ray powder diffraction and revealed that all products were single-phase. As an example we present the Rietveld fit of the X-ray powder diffraction pattern of $\text{Sr}_2[\text{Si}_5\text{N}_8]$ in Fig. 1. The Rietveld refinement of the lattice parameters (space group $Pmn2_1$, no. 31, $a = 571.46(3)$, $b = 682.64(4)$, $c = 934.37(5)$ pm, $wR_p = 0.064$, $R_{F^2} = 0.054$, 17 profile parameters) using the program GSAS [8] was in excellent agreement with the previously published data [6]. Furthermore, the powder diffraction patterns gave no hints on amorphous components in our samples.

The particle sizes of the ground products were estimated by SEM, and were found to range between 0.2 and 0.5 μm with a narrow distribution. The SEM analyses also gave no indication of vitreous phases.

2.2. Optical measurements—the SHEW-method

The SHEW technique is based on the theory of harmonic waves that emanate from the boundary between a linear (here a hemi cylindrical rutile prism) and the nonlinear material under investigation [9]. An incident fundamental wave refracted onto the nonlinear medium induces a nonlinear polarization. The latter radiates a second harmonic wave (SH) in direction Θ_T into the nonlinear medium and in direction Θ_m back into the rutile prism (Fig. 2). Θ_m , which is different from the reflection angle of

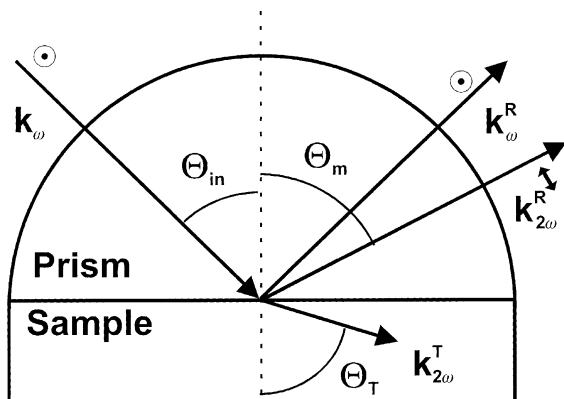


Fig. 2. Experimental setup. The sample powders under investigation are pressed to the flat surface of a hemi cylindrical rutile prism, which can be rotated. The SH signal generated at the interface is emitted under the angle θ_m . In rutile, the refractive index for the detected SH (p-polarized) is smaller (2.67) than that of the s-polarized fundamental (2.74).

the fundamental, is given by Eq. (4)

$$n_p^{2\omega} \sin \theta_m = n_p^\omega \sin \theta_{in} \quad (4)$$

where θ_{in} is the incidence angle of the fundamental beam and $n_p^{2\omega}$ and n_p^ω are the refractive indices of the prism at the two frequencies 2ω and ω , respectively.

For angles θ_{in} smaller than the angle of total reflection the fundamental wave propagates into the nonlinear powder medium and the SH generated by partial phase matching is scattered by the particles and may mask the SH waves from the boundary. The SHEW method reduces this problem by using the evanescent wave generated under total reflection condition with a penetration depth smaller than the coherence length (θ_{in} larger than the total reflection angle). In this case, the incident wave cannot propagate in the powder, the scattered light from phase matched processes is suppressed. The SH waves from the boundary, which are independent of the coherence length, the particle size and the phase matching properties, are observed.

The behavior of electromagnetic waves at boundaries has been described in detail by Bloembergen and Pershan [9]. The SH electric field $E(2\omega)$ from the boundary can be calculated as a function of the angle of incidence θ_{in} [10,11]. It is proportional to $d_{eff} \times E^2(\omega)$, where d_{eff} is the effective second-order susceptibility and $E(\omega)$ is the electrical field incident on the sample (after passing the prism). Inspection of the detailed expressions shows two critical angles of incidence (Eqs. (5) and (6))

$$\sin \theta_{tr} = \frac{n_s^\omega}{n_p^\omega} \quad (5)$$

and

$$\sin \theta_{shtr} = \frac{n_s^{2\omega}}{n_p^\omega} \quad (6)$$

θ_{tr} and θ_{shtr} are the total reflection angles of the fundamental wave and of the second harmonic wave, respectively. n_s^ω and $n_s^{2\omega}$ are the refractive indices of the sample material at the two wavelengths. At angles of incidence θ_{in} larger than both critical angles the SHEW signal is observed. Between the two critical angles the SH signal is only weakly dependent on θ_{in} and exhibits its highest amount. From the height of signal maximum and a fit using the equations of Ref. [11] the effective nonlinear susceptibility can be obtained. For angles larger than the two critical angles the SH signal drops rapidly with increasing angles. At angles smaller than θ_{tr} and θ_{shtr} the signal of the boundary can be masked there by phase matched signal components from the bulk of the nonlinear material and a reliable information on the nonlinearity is not straightforward.

When this method is applied to powders effective nonlinear coefficients are measured, which are averaged over all orientations and which depend on the point group of the sample and on the polarizations of the fundamental and the SH wave. They can be calculated according to Ref. [4]. In a similar way, the refractive indices n_s^ω and $n_s^{2\omega}$ of the birefringent materials have to be averaged.

2.3. Experimental setup

A picosecond Nd:glass laser with a wavelength of 1054 nm and a repetition rate of 8 Hz is used to measure the SH signal emitted from the samples in powder form which is proportional to the Figure of Merit M_{eff} . Single pulses of 2 ps duration and of ~ 2 mJ energy are divided into two parts by a beam splitter. One part generates a SH reference signal in a LiIO_3 single crystal.

For the SHEW experiments the main part of the laser light is focused onto the plane side of the hemi cylindrical rutile (TiO_2) prism (Fig. 2) by a $f = 20$ cm lens. Rutile is well suited for this purpose due to its high refractive index and due to its centrosymmetric space group which does not allow SH generation in the bulk. The polarization of the incident light and the optical axis of the rutile prism are chosen to be parallel to the cylinder axis which is perpendicular to the plane of incidence, e.g. the fundamental was s-polarized. The sample of the nonlinear material is pressed against the flat surface of the prism with a micrometer screw (the pressure was roughly determined to be 10^4 Pa). The reflected SH-signal generated at the boundary between the prism and the sample traverses a polarizer and is detected by a photomultiplier.

The prism holder and the photomultiplier are mounted on rotation stages in order to measure the SH intensity as a function of the angles θ_{in} and θ_m . For each angle of incidence θ_{in} the SH signal is detected as a function of the emission angle to make sure that the intensity maximum at the phase matching angle was detected. This signal and the reference signal were processed by a PC and divided to

Table 1

Averaged figure of merit $M_{\text{eff}} = (d_{\text{eff}}^2)/(n_{2\omega}n_{\omega}^2)$ determined by the SHEW and the Kurtz–Perry method and point group of the investigated samples

Sample	Point group	Space group	Optical axes	n_{ω}	$n_{2\omega}$	M_{eff} (pm ² /V ²) SHEW	M_{eff} (pm ² /V ²) Kurtz–Perry
LiIO ₃	6	$P6_3$ (No. 173)	Uniaxial	1.72	1.90	1.6	1.6
Ba ₂ Si ₅ N ₈	$mm2$	$Pmn2_1$ (No. 31)	Biaxial	–	–	–	0.02
Sr ₂ Si ₅ N ₈	$mm2$	$Pmn2_1$ (No. 31)	Biaxial	2.5	2.6	0.8	0.2
Ca ₂ Si ₅ N ₈	m	Cc (No. 9)	Biaxial	2.55	2.65	0.9	0.04
BaYbSi ₄ N ₇	$6mm$	$P6_3mc$ (No. 186)	Uniaxial	–	–	–	0.02
CeSi ₃ N ₅	222	$P2_12_12_1$ (No. 19)	Biaxial	–	–	–	0.4
KDP	42m	$I\bar{4}2d$ (No. 122)	Uniaxial	1.49	1.51	–	0.02

The refractive indices given result in the best fit. LiIO₃ was used as a reference.

minimize the influence of laser power fluctuations. The angle resolution is set to $\sim 4.5^\circ$ by an aperture in front of the photomultiplier.

For comparison powder experiments according to the Kurtz–Perry method were performed. The laser pulses are focused into a powder sample and the emitted SH signal is measured in a large solid angle. The sample was placed into the focus of a parabolic mirror, so that the emitted light could be efficiently collected and reflected onto a photomultiplier.

3. Results and discussion

The crystal structures of nitridosilicates are built up of three-dimensionally linked SiN₄ tetrahedra in which no inversion centers are present. Therefore, these compounds crystallize in noncentrosymmetric space groups frequently (Table 1). The cations are situated in the voids of the formed three-dimensional network structures. For further details relating to the crystal structures see [6] (Sr₂Si₅N₈ and Ba₂Si₅N₈), [12] (Ca₂Si₅N₈), [13,14] (BaYbSi₄N₇), and [15] (CeSi₃N₅), respectively. The noncentrosymmetric crystal structure is a requirement for a nonzero nonlinearity $\chi^{(2)}$.

With our setup the nonlinear susceptibility is measured relative to a reference sample. We have chosen LiIO₃ powder for reference because of its well-documented literature values of the d_{ijk} coefficients and its rather simple crystal structure. The results of the experiments on LiIO₃ with s-polarized fundamental and p-polarized SH are shown in Fig. 3. One can see the good correspondence of the angle dependence between the measured values (dots) and the theoretical calculations according to the equations in Ref. [11] (line). The angle resolution was taken into account in the theoretical model by performing a convolution of the calculated curve with a Gaussian curve of 4.5° width. From this procedure a fitting parameter is obtained which represents the SH signal for a M_{eff} value of $1.6 \text{ pm}^2/\text{V}^2$ calculated from the d_{ijk} parameters taken from the literature [16] and from the refractive indices [17] averaged over all directions. This fitting parameter is used to determine the M_{eff} values of the other substances from the measured second harmonic signals. A curve similar to that in Fig. 3 is

measured for an s-polarized second harmonic wave, representing a $M_{\text{eff}} = 10.5 \text{ pm}^2/\text{V}^2$. The fitting parameter obtained is the same as that for the p-polarized second harmonic within the experimental error.

Fig. 4 shows experimental data taken on Sr₂Si₅N₈ with s-polarized fundamental wave. The dots represent the data for a p-polarized SH, the triangles stand for an s-polarized SH which was found to be considerably smaller. The polarization dependence of the SH signal is not very surprising since the signal is proportional to an effective nonlinear coefficient which depends on the polarization of the fundamental and the SH wave [4]. To our knowledge, these are the first investigations in which data for both polarization directions are measured and discussed.

A SH signal calculated using the relations in Ref. [11] for p-polarization is shown as a line in Fig. 4. As averaged refractive indices of the sample we have chosen $n_s^\omega = 2.5$, $n_s^{2\omega} = 2.6$ and for the nonlinearity a value of $M_{\text{eff}} = 0.78 \text{ pm}^2/\text{V}^2$ is obtained. Taking into account the angle resolution of our experiment of 4.5° we obtain the solid line, which fits the data points quite well. A more detailed interpretation has to take into account the fact that Sr₂Si₅N₈ is a biaxial crystal with three different wavelength dependent

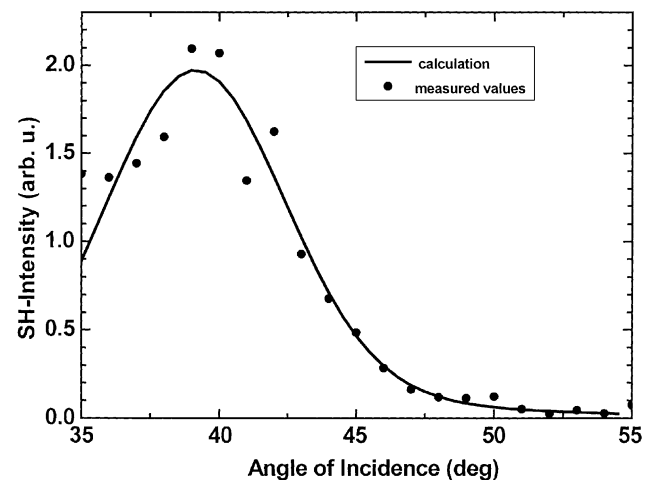


Fig. 3. SHEW data taken on LiIO₃ powder with s-polarized fundamental and p-polarized second harmonic wave. The experimental data are compared with calculations according to Ref. [10] resulting in a fit parameter necessary for the determination of M_{eff} of new materials.

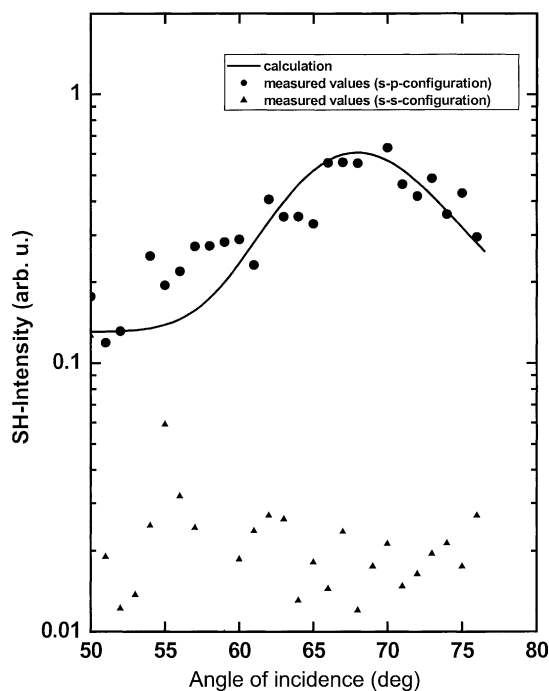


Fig. 4. Experimental SHEW data taken on $\text{Sr}_2\text{Si}_5\text{N}_8$ with s-polarized fundamental wave. The p-polarized second harmonic signal is larger by approximately a factor of 10 than that observed under s-polarization. A comparison with model calculations gives an M_{eff} value for the p-polarized SH-signal of $0.8 \text{ pm}^2/\text{V}^2$. The signal maximum at the large angle of $\sim 70^\circ$ is an indication for refractive indices in the order of 2.5.

refractive indices and a nonlinearity tensor d_{ijk} . Consequently, our model with only one averaged d_{eff} coefficient and just one refractive index for each frequency does not allow a very detailed analysis of the nonlinearity. The signal measured in Fig. 4 is an average over all directions of the single crystallites. Generally, the most accurate information on M_{eff} in SHEW experiments is expected from the decay of the signal at very large angles of incidence [2]. Unfortunately, the indices of refraction of the nitridosilicates are very high (comparable to rutile) and a clear analysis of the decay for $\theta > \theta_{\text{shtr}}, \theta_{\text{fr}}$ is not feasible.

The SH signal generated in s-polarization is found to be smaller approximately by a factor of 10 in Fig. 4 and is close to the sensitivity limit of our system. The signal is too small for a reliable comparison with results of model calculations.

In principle, the $\langle d_{\text{eff}} \rangle$ values for different polarizations can be calculated from the elements of the nonlinear susceptibility tensor taking into account the symmetry of the material [4]. For $\text{Sr}_2\text{Si}_5\text{N}_8$ with $mm2$ symmetry there exist five nonzero coefficients $d_{31}, d_{32}, d_{33}, d_{15}$, and d_{24} which cannot be deduced from the two measured d_{eff} values. Taking into account Kleinman symmetry, the coefficients d_{31} and d_{32} become equal to d_{15} and d_{24} , respectively. A more detailed analysis of d_{eff} according to Ref. [4] shows that it is difficult to find three d -coefficients which are consistent with the experimental findings. There is an indication that the powder consists of irregularly shaped crystallites of nitridosilicates, which do not justify the assumption of an isotropic

distribution of crystal orientations in our sample pressed to the rutile prism. Moreover, the high hardness of the material does not allow to prepare a homogeneous pellet. The surfaces of the crystallites may result in surface enhanced SHG and scattering processes which also affect the measured signal.

We measured SHEW curves for two nitridosilicates. The shapes of the curves are similar to those in Fig. 4 and, in general, we observe a considerably smaller s-polarized SH signal compared to the p-polarized component. This discrepancy seems to result from the anisotropic distribution of the orientations of the crystallites mentioned earlier. Due to their high hardness, the crystallites cannot be crushed by tightening the micrometer screw and thus they do not order randomly. In contrast, softer samples, which can be crushed [2], show a second harmonic of comparable magnitude for both polarizations according to their particular averaged nonlinearities.

The effective nonlinearity M_{eff} , and the averaged refractive indices determined at the fundamental ($\lambda = 1.054 \mu\text{m}$) and the second harmonic frequency ($\lambda = 527 \text{ nm}$) are summarized in Table 1. The SHEW data for the effective second-order susceptibility are compared with the data acquired by the Kurtz–Perry SHG technique [1]. Here, the incident light passed through the sample and the induced SH was emitted in all directions. The results of these experiments are presented in the table, too. They are in agreement with the SHEW-data for $\text{Sr}_2\text{Si}_5\text{N}_8$ which corroborate the findings of the SHEW experiments. It is well known that a more accurate determination of nonlinearities is very difficult: even in single crystals of very good quality the nonlinear properties sensitively depend on details of the growth method giving rise to deviations up to a factor of 2. Moreover, surface induced second harmonic generation contributes to the observed signal [17] and the smoothness of the interface effects the SHG [2].

The larger discrepancy of the results for $\text{Ca}_2\text{Si}_5\text{N}_8$ could be due to the very small amount of substance available for the experiments. A certain amount of sample material is needed to perform reliable SHEW measurements. If the pellet is too thin, it is highly inhomogeneous, cavities emerge and some crystallites are pressed into the rutile prism and the results become irreproducible. Unfortunately, only $\text{Sr}_2\text{Si}_5\text{N}_8$ and $\text{Ca}_2\text{Si}_5\text{N}_8$ were available in sufficient quantities, the others could not be examined with the SHEW technique and are therefore omitted in Table 1. The largest figure of merit M_{eff} is found for $\text{Sr}_2\text{Si}_5\text{N}_8$ in the Kurtz–Perry experiments. From the data in the table no obvious correlation between the point group and the magnitude of the nonlinearity can be deduced.

4. Conclusions

The experiments have shown very high refractive indices and reasonable M_{eff} -values for the new nitridosilicate materials. The effective figure of merit is of the same

order of magnitude as that of LiIO_3 . The extreme hardness of the materials and their presumably high damage threshold make them very attractive for an application in nonlinear optics. Further experiments to examine the phase matching capability in single crystals are necessary. Thus, the relatively high figure of merit M_{eff} values found for nitridosilicates presented in this paper represent a promising starting point for single crystal investigations on these materials. Currently, we are targeting crystal growth techniques for the nitridosilicates. However, experience shows, that this is a long term issue.

References

- [1] S.K. Kurtz, T.T. Perry, A powder technique for the evaluation of nonlinear optical materials, *J. Appl. Phys.* 39 (1968) 3798.
- [2] M. Kiguchi, M. Kato, N. Kumegawa, Y. Taniguchi, Technique for evaluating second-order nonlinear optical materials in powder form, *J. Appl. Phys.* 75 (1994) 4332.
- [3] R. Kremer, A. Boudrioua, J.C. Loulergue, A. Iltis, Effective nonlinear coefficients of organic powders measured by second-harmonic generation in total reflection: numerical and experimental analysis, *J. Opt. Soc. Am. B* 16 (1999) 83.
- [4] S.J. Cyvin, J.E. Rauch, J.C. Decius, *J. Chem. Phys.* 43 (1965) 4083.
- [5] H. Lange, G. Wötting, G. Winter, Silicon nitride—from powder to the ceramic material, *Angew Chem. Int. Ed. Engl.* 30 (1991) 1579.
- [6] T. Schlieper, W. Milius, W. Schnick, Nitrido-silicates. II. High-temperature syntheses and crystal structures of $\text{Sr}_2\text{Si}_5\text{N}_8$ and $\text{Ba}_2\text{Si}_5\text{N}_8$, *Z. Anorg. Allg. Chem.* 621 (1995) 1380.
- [7] W. Schnick, H. Huppertz, R. Lauterbach, High-temperature syntheses of novel nitrido- and oxonitridosilicates and sialons using RF furnaces, *J. Mater. Chem.* 9 (1999) 289.
- [8] R.B. von Dreele, A.C. Larson, General structure analysis system, Los Alamos Natl Lab. Rep. LAUR (1990) 86–748.
- [9] N. Bloembergen, P.S. Pershan, Light waves at the boundary of nonlinear media, *Phys. Rev.* 128 (1962) 606.
- [10] N. Bloembergen, C.H. Lee, Total reflection in second harmonic generation, *Phys. Rev. Lett.* 15 (1967) 835.
- [11] A. Le Calvez, E. Freysz, A. Ducasse, Second harmonic field generated in reflection by an inhomogeneous nonlinear polarization, *Opt. Commun.* 145 (1998) 135.
- [12] T. Schlieper, W. Schnick, Nitrido-silicates. I. High-temperature synthesis and crystal structure of $\text{Ca}_2\text{Si}_3\text{N}_8$, *Z. Anorg. Allg. Chem.* 621 (1995) 1037.
- [13] H. Huppertz, W. Schnick, $\text{BaYbSi}_4\text{N}_7$ —unexpected structural possibilities in nitridosilicates, *Angew. Chem. Int. Ed. Engl.* 35 (1996) 1983.
- [14] H. Huppertz, W. Schnick, Crystal structure, and properties of the nitrido silicates $\text{SrYbSi}_4\text{N}_7$ and $\text{BaYbSi}_4\text{N}_7$, *Z. Anorg. Allg. Chem.* 623 (1997) 212.
- [15] M. Woike, W. Jeitschko, Crystal structure of cerium silicon nitride (1/3/5), CeSi_3N_5 , *Z. Kristallogr.* 211 (1996) 813.
- [16] V.G. Dmitriev, G.G. Gurzadyan, D.N. Nikogosyan, *Handbook of Nonlinear Optical Crystals*, Springer, Berlin, 1997.
- [17] R.L. Sutherland, *Handbook of Nonlinear Optics*, Marcel Dekker, New York, 1996, (Chapter 5).